AN ANALYSIS OF CURVED FLOW WIND TUNNEL TESTING

by

Mack Steele Mutchler

Thesis submitted to the Graduate Faculty of the

Virginia Polytechnic Institute and State University

in partial fulfillment of the requirements for the degree of

MASTER OF SCIENCE

in

Aerospace Engineering

APPROVED:

F. H. Lutze, Chairman

J. A. Schetz

E. M. Cliff

July, 1974

Blacksburg, Virginia

ACKNOWLEDGEMENTS

The author wishes to express his appreciation to the National Aeronautics and Space Administration for sponsorship of this work through Task Order . He also wishes to thank of the Aerospace and Ocean Engineering Department of Virginia Polytechnic Institute and State University for his comments and advice in the preparation of this thesis.

TABLE OF CONTENTS

LIST OF FIGURES

NOMENCLATURE

A, B, C	twenty-four constants which depend on the shape
A_1, B_1, C_1	and orientation of the body, and defined by
A', B', C'	equations 21, 23, 36 or are always zero for a
F', G', H'	symmetric body
F'', G'', H''	
F''', G''', H'''	
P', Q', R'	
P'', Q'', R''	
$\overline{A}$	the eigenvector
a	the real part of the eigenvalue
a_r	radial acceleration
b	wing span
C_n	coefficient of the yawing moment
C_{nr}	$\dfrac{\partial C_n}{\partial \frac{rb}{2V}}$
$C_{n\dot{r}}$	$\dfrac{\partial C_n}{\partial \frac{\dot{r}b}{2V}}$
$C_{n\beta}$	$\dfrac{\partial C_n}{\partial \beta}$
$C_{n\dot{\beta}}$	$\dfrac{\partial C_n}{\partial \frac{\dot{\beta}b}{2V}}$
F_n	defined where used (see equations 34 and 45)
H	total pressure

h	height used to describe the size of a fluid element
I_x, I_y, I_z	moments of inertia about the body
i	$\sqrt{-1}$
K	kinetic energy of the fluid when the body is stationary
K_1, K_2, K_3	mass coefficients
K_1', K_2', K_3'	inertia coefficients
L, M, N	moments in the body axis system (see figure 5)
L_1, M_1, N_1	moments in the wind axis system (see figure 3)
M_ψ	yawing moment due to the flexures
l, m, n	direction cosines describing the orientation of the body with respect to the wind axis
P	static pressure
p, q, r	angular velocities of a body
$\bar{q}$	dynamic pressure; $\frac{1}{2}\rho V^2$
R	radial distance from the center of curvature
$\hat{r}$	non-dimensional yawing rate
S	surface area of the body
s	reference area of the body (usually the wing area)
T	kinetic energy of the system
t	time
$t_{\frac{1}{2}}$	time to ½ the amplitude
u, v, w	velocity components
V	velocity
V'	volume
X, Y, Z	forces in the body-axis system (see figure 5)

X_1, Y_1, Z_1	forces in the wind axis system (see figure 3)
x, y, z	coordinates of the body or a point on the body
α	angle of attack
β	angle of sideslip
θ	angle used to describe the size of a fluid element
λ	the eigenvalue
ρ	density
ϕ_1, ϕ_2, ϕ_3	functions of the shape of the body in the flow
ϕ_4, ϕ_5, ϕ_6	
ψ	flight path angle; equals $-\beta$ in the wind tunnel
Ω	angular velocity of the flow
ω	the imaginary part of the eigenvalue

Subscripts and Superscripts

c	the center of the wind tunnel
$\cdot$	time derivative

I. INTRODUCTION

In the early stages of development of an aircraft, it is important to determine the aerodynamic stability derivatives, both static and dynamic, in order to be able to predict the stability and handling characteristics of that aircraft. In recent years, a considerable amount of attention has been given to the problem of determining the dynamic or more specifically the so-called rotary stability derivatives. The interest in this aspect of the problem is primarily due to the need to predict the spin characteristics of aircraft of modern design. Currently the primary method used to predict the aerodynamic stability derivatives is that of testing a model of the aircraft of interest in a wind tunnel.[1]

The rotary derivatives may be determined in the wind tunnel by oscillating the flow or the model in either roll, pitch or yaw. Unfortunately, unsteady aerodynamic effects are present in this type of test and in many cases they are not small, making the extraction of pure rotary derivatives difficult if not impossible. No completely satisfactory method has of yet been developed for separating or even estimating these derivatives without loss of accuracy in most cases. An alternative approach, developed in the 1940's at Langley Research Center, has been used to obtain pure rotary derivatives. In this method, referred to as the method of curved flow, the model is immersed in a curved flow with a non-uniform velocity profile which simulates flight

in a curved path. Such a flow is steady, but still contains the desired rotary motion.[2]

This paper provides the reader with the information and theory needed to understand and use curved flow wind tunnel testing. The principles involved in several other methods of testing are discussed so that a comparison may be made with the curved flow method with emphasis being placed on the oscillating model method. The results obtained for the dynamic stability derivatives from a twin engine fighter aircraft, known as the F-4 Phantom, that was tested in the Stability Wind Tunnel at Virginia Polytechnic Institute and State University using the curved flow technique is also presented.

II. THEORY OF CURVED FLOW WIND TUNNEL TESTING

2.1. Basic Principles of the Curved Flow Wind Tunnel

When a body of some finite size moves in a curved path about some point this body experiences a distribution of the velocity proportional to the distance from the point about which it is moving. If the body is held stationary and the fluid is forced to move over the body in the same manner as when the body moved through the air, then the distribution in velocity may be expressed in equation form as (see figure 1)

$$V = R\Omega \tag{1}$$

Where Ω, the constant of proportionality, is just the angular velocity of the fluid motion and R is the radial distance from the center of rotation. This relationship must also hold true in curved flow if a true simulation is to be achieved. If the angular velocity of the flow is assumed equal to the angular rate of the body and in addition the planar motion described in equation 1 is chosen to be about the x axis then the derivatives obtained will be the yawing (or r) derivatives. It is possible to limit the discussion to motion about the z axis since an analysis of planar motion about the x or y axes would be similar. Thus the equation above for the velocity may be rewritten for the motion about the z axis by substituting the angular rate, r, for the angular velocity, Ω.

$$V = Rr \tag{2}$$

Dynamic pressure is used in wind tunnels as a means of measuring the velocity of the flow. It has been seen above that the velocity for curved flow will vary across the wind tunnel. Thus some average value of velocity and dynamic pressure would have to be used to describe the velocity in the curved flow wind tunnel. It is convenient to use the velocity at the centerline of the tunnel as the tunnel speed and to record the reference dynamic pressure at that point. This can be written as

$$\overline{q}_c = \tfrac{1}{2}\rho R^2 r^2 \Big|_c \tag{3}$$

The non-dimensional yawing rate is defined for curved wind tunnel flow to be

$$\hat{r} = \frac{rb}{2V}\Big|_c \tag{4}$$

which when the velocity in 4 is replaced by equation 2 the non-dimensional yawing rate becomes

$$\hat{r} = \frac{b}{2R}\Big|_c \tag{5}$$

The theory presented thus far shows that the non-dimensional yawing rate is independent of the velocity of the motion for a given wind tunnel curvature. This is true only when the assumption of equality between Ω, the angular velocity of the fluid motion and r, the yawing angular rate is valid. Such an assumption requires that the viscosity and any higher ordered effects be neglected.

When a fluid is forced to move in a curved path as it is in curved flow wind tunnel tests, every element of the fluid must experience a

force causing it to move in a curved path. This force is provided by a static pressure gradient in the radial direction. This radial pressure gradient is the primary difference between curved flow moving over a stationary body and the flow over a body that is moving in a curved path since the latter experiences a zero static pressure gradient.

The pressure gradient which exists in the tunnel can be determined by applying Newton's Laws to a small element of fluid. Consider such an element of fluid located at a distance R from the center of rotation of the flow. Let the dimensions of the element be ΔR, $R\Delta\theta$ and Δh (see figure 2) and the density be ρ. The mass can therefore be given by

$$M = \rho \Delta R \Delta h R \Delta\theta \tag{6}$$

The acceleration in the radial direction is given by the well known expression

$$a_r = \frac{-V^2}{R} \tag{7}$$

From equation 2 the velocity about the z rotational axis may be used in equation 7 above to give

$$a_r = -Rr^2 \tag{8}$$

The relationship for the pressure gradient can then be obtained by applying Newton's Second Law in the radial direction or

$$-\Delta P \Delta h R \Delta\theta = -\rho \Delta R \Delta h \Delta\theta R^2 r^2$$

$$\Delta P = \rho R \Delta R r^2 \tag{9}$$

$$\frac{\Delta P}{\Delta R} = \rho R r^2$$

By making the fluid element very small (i.e. taking the limit as ΔR approaches zero) an expression may be derived to describe how the static pressure must change with respect to the radial distance in terms of the distance from the center of curvature.

$$\frac{dp}{dR} = \rho R r^2 \tag{10}$$

The above equation may be integrated along a path perpendicular to the circular path of the flow (r is assumed constant throughout the flow) and the constant of integration may be evaluated at the center of the tunnel. This may then be non-dimensionalized by the use of the dynamic pressure at the center of the tunnel to obtain

$$P-P_c = \rho r^2 \frac{R^2-R_c^{\,2}}{2}$$

$$\frac{P-P_c}{q_c} = \frac{R^2-R_c^{\,2}}{R_c^{\,2}} \tag{11}$$

Furthermore, it may be easily seen that the distribution in the static pressure and the distribution in the dynamic pressure are equal.

$$\frac{\bar{q}-\bar{q}_c}{\bar{q}_c} = \frac{R^2-R_c^{\,2}}{R_c^{\,2}} \tag{12}$$

Therefore each is half of the distribution of the total pressure.

$$\frac{H-H_c}{q_c} = \frac{2(R^2-R_c^{\,2})}{R_c^{\,2}} \tag{13}$$

By taking the derivative of the total pressure distribution with respect to the radial distance, R, it is observed that by using equation 5, one

may obtain an expression for the non-dimensional yawing rate in terms of the derivative of the total head distribution evaluated at the center of the tunnel.

$$\hat{r} = \frac{b}{2R} \tag{5}$$

$$\frac{d}{dR}\,\frac{H-H_c}{q_c} = \frac{4R}{R_c^{\,2}}$$

$$\hat{r}_c = \frac{b}{8}\,\frac{d}{dR}\left[\frac{H-H_c}{q_c}\right]\Bigg|_c \tag{14}$$

Equations 2 and 14 are the basic relations used to calibrate the wind tunnel for some prescribed value of the non-dimensional yawing rate. In general, the calibration for $\hat{r}_c$ would remain the same for every velocity. However the effect of viscosity and tunnel irregularities require the measurement of the total pressure gradient to be made for each velocity required in the test since there is a slight variation in the yawing rate due to the velocity. The gradient measurements are used in equation 14 to determine the non-dimensional yaw rate, $\hat{r}_c$, for each tunnel curvature and speed.

2.2 Reactions On the Body in Curved Flow

Unfortunately, the flow patterns in the curved flow tunnel and in curved flight are not exactly the same. The greatest difference is that of the static pressure gradient in the wind tunnel but, another difference is the rotationality of the flow resulting from the addition of the drag screens, necessary to give the total pressure and velocity distributions described in equations 14 and 2. This rotationality makes the flow in the wind tunnel a non-potential type of flow in which the total pressure

varies from streamline to streamline. The flow for curved flight, on the other hand, is an irrotational, potential flow. If it may be assumed that the body is very small when compared to the radius of curvature of the flow, then the force on the body due to a non-potential flow would be approximately the same as the force on a body due to a potential flow. Thus a potential flow formulation of the forces and moments experienced by the body may be used with reasonable accuracy. This method of formulation was first derived by G. I. Taylor in reference 3.

The only important difference left unresolved is the forces due to the static pressure gradient. Consider a body in curved flow at a fixed angle of attack, α, and a fixed angle of sideslip, β. Assume that the body is symmetrical with a set of body axes located such that the center of volume of the body is the origin of the axes (see figure 3). Lord Kelvin found that the kinetic energy of a system in which curving flow is moving past a spherical body with body velocity components $\dot{x}$, $\dot{y}$ and $\dot{z}$ is[4]

$$2T = (M+\tfrac{1}{2}\rho V')(\dot{x}^2+\dot{y}^2+\dot{z}^2) + 2\ K \tag{15}$$

where M is the mass of the sphere, V' is its volume and the quantities ρ and K are the density and kinetic energy of the fluid when the body is held stationary. A method for finding the value of K was next developed by Sir Horace Lamb.[4] He assumed that if the mass of the spherical body was made equal to the mass of the displaced fluid and the body was made to move with the fluid in its neighborhood, then the kinetic energy would be the same as if there were no body present.

$$2K = \text{constant} - 3/2\ \rho v(u^2+v^2+w^2) \tag{16}$$

Where u, v and w are the components of the velocity of the fluid before the spherical body has been introduced. To apply this method to arbitrarily shaped bodies, Lamb assumed a velocity potential of the form

$$\phi = u\phi_1 + v\phi_2 + w\phi_3 + p\phi_4 + q\phi_5 + r\phi_6 \tag{17}$$

where u, v, w, p, q and r are the velocities and angular rates and ϕ_1, ϕ_2, ϕ_3, ϕ_4, ϕ_5 and ϕ_6 are functions of the shape of the body in the flow. The kinetic energy of the fluid may be found from

$$\frac{2T}{\rho} = -\iint \phi \frac{\partial\phi}{\partial n} dS \tag{18}$$

where the integration above is over the surface of the arbitrarily shaped body. Performing the above integration over the body surface in an infinite irrotational fluid, initially at rest, Lamb obtained[4]

$$\begin{aligned} \frac{2T}{\rho} = {} & A_1u^2 + B_1v^2 + C_1w^2 + 2A'vw + 2B'wu + 2C'uv + P'p^2 + Q'q^2 + \\ & R'r^2 + 2P''qr + 2Q''rp + 2R''pq + 2p(F'u + G'v + H'w) + \\ & 2q(F''u + G''v + H''w) + 2r(F'''u + G'''v + H'''w) \end{aligned} \tag{19}$$

where the twenty-one constants are integrals of the surface shape and orientation of the body. Since the body is immersed in curved flow and does not rotate, p = q = r = 0, and equation 19 becomes

$$\frac{2T}{\rho} = A_1u^2 + B_1v^2 + C_1w^2 + 2A'vw + 2B'wu + 2c'uv \tag{20}$$

where A_1, B_1, C_1, A', B' and C' are of the form

$$
\begin{aligned}
A_1 &= \iint \phi_1 l ds \\
B_1 &= \iint \phi_2 m ds \\
C_1 &= \iint \phi_3 n ds \\
A' &= \iint \phi_2 n ds = \phi_3 m ds \\
B' &= \iint \phi_1 n ds = \phi_3 l ds \\
C' &= \iint \phi_1 m ds = \phi_2 l ds
\end{aligned}
\tag{21}
$$

and l, m and n are direction cosines with respect to the body fixed coordinate axis system in which the x axis is aligned with the flow. In reference 5, Donlan derived relations for the above six symmetric and asymmetric coefficients in terms of three symmetric coefficients. The relations are

$$
\begin{aligned}
A_1 &= A\cos^2\beta\cos^2\alpha + B\sin^2\beta + C\sin^2\alpha\cos^2\beta \\
B_1 &= A\cos^2\alpha\sin^2\beta + B\cos^2\beta + C\sin^2\alpha\sin^2\beta \\
C_1 &= A\sin^2\alpha + C\cos^2\alpha \\
A' &= (C-A)\sin\alpha\sin\beta\cos\beta \\
B' &= (C-A)\sin\alpha\cos\alpha\cos\beta \\
C' &= -(C-A)\cos^2\alpha\sin\beta\cos\beta + (C-B)\sin\beta\cos\beta
\end{aligned}
\tag{22}
$$

where the constants A, B and C are

$$
\begin{aligned}
A &= K_1 V' \\
B &= K_2 V' \\
C &= K_3 V'
\end{aligned}
\tag{23}
$$

and K_1, K_2, and K_3 are inertia coefficients for an ellipsoid of revolution taken to approximate the actual arbitrary shape of the body. These

values can be obtained from figure 4. Equation 15 may now be written for an arbitrarily shaped body in the form of equation 16 as

$$\frac{2K}{\rho} = \text{constant} - V'(u^2+v^2+w^2) - \frac{2T}{\rho} \tag{24}$$

Again following the example of Lamb[4], and Taylor[3] the forces and moments on a body are due to the fluctuations in the energy of the flow about the body. These force and moment equations are

$$\begin{aligned}
x_1 &= \frac{-\partial K}{\partial x} = \tfrac{1}{2}\rho\, V'\frac{\partial}{\partial x}(u^2+v^2+w^2) + \frac{\partial T}{\partial u}\frac{\partial u}{\partial x} + \frac{\partial T}{\partial v}\frac{\partial v}{\partial x} + \frac{\partial T}{\partial w}\frac{\partial w}{\partial x} \\
y_1 &= \frac{-\partial K}{\partial y} = \tfrac{1}{2}\rho\, V'\frac{\partial}{\partial y}(u^2+v^2+w^2) + \frac{\partial T}{\partial u}\frac{\partial u}{\partial y} + \frac{\partial T}{\partial v}\frac{\partial v}{\partial y} + \frac{\partial T}{\partial w}\frac{\partial w}{\partial y} \\
z_1 &= \frac{-\partial K}{\partial z} = \tfrac{1}{2}\rho\, V'\frac{\partial}{\partial z}(u^2+v^2+w^2) + \frac{\partial T}{\partial u}\frac{\partial u}{\partial z} + \frac{\partial T}{\partial v}\frac{\partial v}{\partial z} + \frac{\partial T}{\partial w}\frac{\partial w}{\partial z} \\
L_1 &= w\frac{\partial T}{\partial v} - v\frac{\partial T}{\partial w} \\
M_1 &= u\frac{\partial T}{\partial w} - w\frac{\partial T}{\partial u} \\
N_1 &= v\frac{\partial T}{\partial u} - u\frac{\partial T}{\partial v}
\end{aligned} \tag{25}$$

Since the coordinate system for the above equations was chosen such that the x axis was aligned with the flow (see figure 3), $v = w = 0$, equation 25 becomes

$$\begin{aligned}
x_1 &= \tfrac{1}{2}\rho V'\frac{\partial}{\partial x}(u^2) + \frac{\partial T}{\partial u}\frac{\partial u}{\partial x} + \frac{\partial T}{\partial v}\frac{\partial v}{\partial x} + \frac{\partial T}{\partial w}\frac{\partial w}{\partial x} \\
y_1 &= \tfrac{1}{2}\rho V'\frac{\partial}{\partial y}(u^2) + \frac{\partial T}{\partial u}\frac{\partial w}{\partial y} + \frac{\partial T}{\partial v}\frac{\partial v}{\partial y} + \frac{\partial T}{\partial w}\frac{\partial w}{\partial y}
\end{aligned} \tag{26}$$

$$z_1 = \tfrac{1}{2}\rho V' \frac{\partial}{\partial z}(u^2) + \frac{\partial T}{\partial u}\frac{\partial w}{\partial z} + \frac{\partial T}{\partial v}\frac{\partial v}{\partial z} + \frac{\partial T}{\partial w}\frac{\partial w}{\partial z}$$

$$L_1 = 0$$

$$M_1 = u\frac{\partial T}{\partial w} \tag{26}$$

$$N_1 = -u\frac{\partial T}{\partial v}$$

The total pressure, H, for incompressible, fluids can be written as

$$H = p + \tfrac{1}{2}\rho V^2 \tag{27}$$

where p is the static pressure and V, the velocity, is equal to u. In equation 13, the total pressure was shown to vary in the radial direction. Since the x axis is aligned with the flow, $\frac{\partial H}{\partial x}$ and $\frac{\partial H}{\partial z}$ will be zero but $\frac{\partial H}{\partial y}$ will not be zero. However, $\frac{\partial H}{\partial y}$ may be assumed to be zero since this assumption is of the order of the irrotationality of the flow assumption.

$$\frac{\partial H}{\partial x} = \frac{\partial p}{\partial x} + \rho u \frac{\partial u}{\partial x} = 0$$

$$\frac{\partial H}{\partial y} = \frac{\partial p}{\partial y} + \rho u \frac{\partial u}{\partial y} \cong 0 \tag{28}$$

$$\frac{\partial H}{\partial z} = \frac{\partial p}{\partial z} + \rho u \frac{\partial u}{\partial z} = 0$$

Using these equations with the requirements for irrotationality of the flow the following relations may be derived.

$$\rho u \frac{\partial u}{\partial x} = -\frac{\partial p}{\partial x} \tag{29}$$

$$\rho u \frac{\partial u}{\partial y} = \rho u \frac{\partial v}{\partial x} = - \frac{\partial p}{\partial y}$$

$$\rho u \frac{\partial u}{\partial z} = \rho u \frac{\partial w}{\partial x} = - \frac{\partial p}{\partial z} \tag{29}$$

Equation 20 yields the following equations

$$\frac{\partial T}{\partial u} = \rho A_1 u + \rho B' w + \rho C' v$$

$$\frac{\partial T}{\partial v} = \rho B_1 v + \rho A' w + \rho C' u \tag{30}$$

$$\frac{\partial T}{\partial w} = \rho C_1 w + \rho A' v + \rho B' u$$

and with the fact that $v = w = 0$, they reduce to

$$\frac{\partial T}{\partial u} = \rho A_1 u$$

$$\frac{\partial T}{\partial v} = \rho C' u \tag{31}$$

$$\frac{\partial T}{\partial w} = \rho B' u$$

Making use of equations 29 and 31, equations 26 become

$$X_1 = - (V'+A_1) \frac{\partial P}{\partial x} - C' \frac{\partial P}{\partial y} - B' \frac{\partial P}{\partial z}$$

$$Y_1 = - (V'+A_1) \frac{\partial P}{\partial y} + \rho C' u \frac{\partial v}{\partial y} + \rho B' u \frac{\partial w}{\partial y} \tag{32}$$

$$Z_1 = - (V'+A_1) \frac{\partial P}{\partial z} + \rho C' u \frac{\partial v}{\partial z} + \rho B' u \frac{\partial w}{\partial z}$$

$$L_1 = 0$$

$$M_1 = \rho B' u^2$$
$$N_1 = -\rho C' u^2 \tag{32}$$

Since the flow is curved about the vertical axis only, and is in the direction of the x axis, $\frac{\partial v}{\partial z} = \frac{\partial w}{\partial z} = \frac{\partial v}{\partial y} = \frac{\partial w}{\partial y} = \frac{\partial p}{\partial x} = \frac{\partial p}{\partial z} = 0$. Therefore equation 32 reduces to

$$X_1 = -C' \frac{\partial P}{\partial y}$$

$$Y_1 = -(V' + A_1) \frac{\partial P}{\partial y}$$

$$Z_1 = 0$$

$$L_1 = 0 \tag{33}$$

$$M_1 = \rho B' u^2$$

$$N_1 = -\rho C' u^2$$

Using the relations in equations 22 and 23, and rotating from the wind axis system to the body axis system, the above equations become

$$\text{Axial Force} = \{-(1+K_2) \sin\beta \cos\alpha + F_n \cos\beta \cos\alpha\}(\frac{\partial P}{\partial y})(V')$$

$$\text{Side Force} = \{-(1+K_1 \cos^2\alpha + K_3 \sin^2\alpha) \cos\beta - F_n \sin\beta\}(\frac{\partial P}{\partial y})(V') \tag{34}$$

$$\text{Normal Force} = \{-(1+K_2) \sin\beta \sin\alpha + F_n \cos\beta \sin\alpha\}(\frac{\partial P}{\partial y})(V')$$

$$\text{Rolling Moment} = \{\tfrac{1}{2}\rho u^2 (K_2 - K_3) \sin 2\beta \sin\alpha\}(V')$$

$$\text{Pitching Moment} = \{\tfrac{1}{2}\rho u^2(K_3-K_1)\ \sin 2\alpha\ \cos^2\beta\}(V')$$
$$\text{Yawing Moment} = \{\tfrac{1}{2}\rho u^2(K_1-K_2)\ \sin 2\beta\ \sin\alpha\}(V') \tag{34}$$

where

$$F_n = \{(K_3-K_1)\ \cos^2\alpha + (K_2-K_3)\}\ \sin 2\beta$$

2.3. Reactions on the Body in Curved Flight

Curved flight involves the motion of a solid through what may be considered an infinite fluid. If one assumes that the motion of the fluid is due only to the effect of the motion of the solid, then the fluid will be irrotational and can therefore be represented by the use of a velocity potential, ϕ, that satisfies the continuity equation.[4] The equation for this potential is the same as for the curved flow case and is equation 15.

If the motion of the fluid at some instant is assumed to be generated by an impulsive force, the energy that the solid body imparts to the fluid by merely moving through the fluid will be the same equation that was found for curved flow,[4] where as before, the twenty-one constants are functions of the slope and orientation of the body. If the body is assumed to be symmetrical about each of its three mutually perpendicular axes then the above equations would simplify to

$$2T/\rho = Au^2 + Bv^2 + Cw^2 + P'p^2 + Q'q^2 + R'r^2 \tag{35}$$

where this equation differs from equation 20 in that the above equation allows the body to rotate and that the coordinate axes for the above

equation is aligned with the symmetrical axes of the body (see figure 5). A, B and C are the same as in equation 23 and P', Q' and R' are as follows

$$
\begin{aligned}
P' &= \iint \phi_4 \, (ny - mz) \, dS = K_1' I_x \\
Q' &= \iint \phi_5 \, (lz - nx) \, dS = K_2' I_y \\
R' &= \iint \phi_6 \, (mx - ly) \, dS = K_3' I_z
\end{aligned}
\tag{36}
$$

where as in equation 21, l, m and n are the direction cosined, x, y and and z are the coordinates of points on the body surface, K_1', K_2' and K_3' are inertia coefficients obtained from Figure 6 and I_x, I_y and I_z are the moments of inertia of the body.

Lamb, in reference 4, gave the equations of motion for a body with angular velocities p, q and r, translational velocities u, v and w and moving under the action of a set of external forces and moments in Lagrangian form. Writing the equations for the axis system shown in figure 5, one obtains

$$
\begin{aligned}
X &= \frac{-d}{dT} \frac{\partial T}{\partial u} + r \frac{\partial T}{\partial v} - q \frac{\partial T}{\partial w} \\
Y &= \frac{-d}{dT} \frac{\partial T}{\partial v} + p \frac{\partial T}{\partial w} - r \frac{\partial T}{\partial u} \\
Z &= \frac{-d}{dT} \frac{\partial T}{\partial w} + q \frac{\partial T}{\partial u} - p \frac{\partial T}{\partial v} \\
L &= \frac{-d}{dT} \frac{\partial T}{\partial p} + w \frac{\partial T}{\partial v} - v \frac{\partial T}{\partial w} + r \frac{\partial T}{\partial q} - q \frac{\partial T}{\partial r} \\
M &= \frac{-d}{dT} \frac{\partial T}{\partial q} + u \frac{\partial T}{\partial w} - w \frac{\partial T}{\partial u} + p \frac{\partial T}{\partial r} - r \frac{\partial T}{\partial p} \\
N &= \frac{-d}{dT} \frac{\partial T}{\partial r} + v \frac{\partial T}{\partial u} - u \frac{\partial T}{\partial v} + q \frac{\partial T}{\partial p} - p \frac{\partial T}{\partial q}
\end{aligned}
\tag{37}
$$

If we restrict our examination to the steady condition of rotating about a vertical axis ($q = 0$), the above equations reduce to

$$
\begin{aligned}
X &= r \frac{\partial T}{\partial v} \\
Y &= p \frac{\partial T}{\partial w} - r \frac{\partial T}{\partial u} \\
Z &= -p \frac{\partial T}{\partial v} \\
L &= w \frac{\partial T}{\partial v} - v \frac{\partial T}{\partial w} \\
M &= u \frac{\partial T}{\partial w} - w \frac{\partial T}{\partial u} + p \frac{\partial T}{\partial r} - r \frac{\partial T}{\partial p} \\
N &= v \frac{\partial T}{\partial u} - u \frac{\partial T}{\partial v}
\end{aligned}
\tag{38}
$$

Using equation 35 the partial derivatives may be evaluated and using an angular transformation about the y axis the p and r angular rates may be evaluated (see figure 5).

$$
\begin{aligned}
r &= -\Omega \cos\alpha \\
p &= \Omega \sin\alpha
\end{aligned}
\tag{39}
$$

to yield

$$
\begin{aligned}
X &= -\rho B v \Omega \cos\alpha \\
Y &= \rho C w \Omega \sin\alpha + \rho A u \Omega \cos\alpha \\
Z &= -\rho B v \ell \sin\alpha \\
L &= \rho (B-C) w v \\
M &= \rho (C-A) u w + \tfrac{1}{2}\rho\Omega^2 (P'-R') \sin 2\alpha
\end{aligned}
\tag{40}
$$

An examination of figure 5 yields the following relations.

$$u = V \cos\alpha \cos\beta$$
$$v = V \sin\beta$$
$$w = V \sin\alpha \cos\beta \qquad (41)$$
$$\Omega = \frac{V}{R} \text{ (from equation 1)}$$

Using equations 23, 36 and 41, equation 40 may be written in the following way.

$$\text{Axial Force} = \rho \frac{V^2}{R} K_2 (V') \sin\beta \cos\alpha$$

$$\text{Side Force} = \rho \frac{V^2}{R} K_1 (V') \cos\beta \cos^2\alpha + \rho \frac{V^2}{R} K_3 (V') \cos\beta \sin^2\alpha$$

$$\text{Normal Force} = \rho \frac{V^2}{R} K_2 (V') \sin\beta \sin\alpha$$

$$\text{Rolling Moment} = \tfrac{1}{2}\rho V^2 (K_2 - K_3) (V') \sin 2\beta \sin\alpha \qquad (42)$$

$$\text{Pitching Moment} = \tfrac{1}{2}\rho V^2 (K_3 - K_1) (V') \sin 2\alpha \cos^2\beta + \tfrac{1}{2}\rho \frac{V}{R}^2 (K_1' I_x - K_3' I_z) \sin 2\alpha$$

$$\text{Yawing Moment} = \tfrac{1}{2}\rho V^2 (K_1 - K_2) V' \sin 2\beta \cos\alpha$$

2.4. Corrections to the Test Results

The corrections for the wind tunnel can be obtained by subtracting the predicted forces and moments for curved flow from the predicted forces and moments for curved flight. These corrections can thus be added to the results from the test of an aircraft to obtain the proper values of the forces and moments and thus determine the proper values of the stability derivatives.

Since for the curved flow case and the curved flight case the y axis was in the radial direction, the following is identically true.

$$\frac{\partial P}{\partial y} = \frac{\partial P}{\partial R} \tag{43}$$

From equations 2 and 10 it may be seen that

$$\frac{\partial P}{\partial R} = \frac{\rho V^2}{R} \tag{44}$$

Therefore by performing the operations described above the corrections become

$$\text{Axial Force Correction} = \{(1+2K_2)\sin\beta\cos\alpha - F_n\cos\beta\cos\alpha\}\frac{\partial P}{\partial R}(V')$$

$$\text{Side Force Correction} = \{(1+2K_1\cos^2\alpha + 2K_3\sin^2\alpha)\cos\beta + F_n\sin\beta\}\frac{\partial P}{\partial R}(V')$$

$$\text{Normal Force Correction} = \{(1+2K_2)\sin\beta\sin\alpha - F_n\cos\beta\sin\alpha\ \frac{\partial P}{\partial R}(V')$$

$$\text{Rolling Moment Correction} = 0$$

$$\text{Pitching Moment Correction} = \tfrac{1}{2}\rho\frac{V}{R}^2(K_1'Ix - K_3'Iz)(V')\sin 2\alpha \tag{45}$$

$$\text{Yawing Moment Correction} = 0$$

where as before

$$F_n = \{(K_3-K_1)\cos^2\alpha + (K_2-K_3)\}\sin 2\beta$$

2.5. Physical Setup and Procedure Used in Curved Flow Testing

Curved flow testing has as its goal the determination of the rotary stability derivatives. In order to determine these derivatives one would want to test a specific model in at least two values of

curvature. The non-dimensional forces and moments obtained for each curvature may then be plotted versus the non-dimensional yawing rate, for example. The slope which is the value of the stability derivative in question may then be measured.

The first step in planning a curved flow test is to choose the values of curvature. Appendix A reproduces six tables from reference 6 for the curvatures obtainable in the Stability Wind Tunnel at Virginia Polytechnic Institute and State University. These tables were obtained at the time the tunnel was built by calculating the approximate curvature and then adding wires to screens at the upstream end on a trial and error basis until the equations and relations presented above were satisfied. Since the velocity of the flow and tunnel wall irregularities have an effect on the non-dimensional yawing rate, $\hat{r}$, a survey of the static and total pressures across the tunnel should be performed at the beginning of a curved flow test to obtain an accurate value of the yawing rate for that curvature. Equation 14 is used in the above process for determining $\hat{r}$.

In section 2.4, the corrections for the forces and moments have been obtained. Since the body in that analysis was an ellipsoid of revolution with mass coefficients K_1, K_2 and K_3, inertia coefficients K_1', K_2' and K_3', moments of inertia I_x, I_y and I_z and a volume, V', the body tested should be approximated by such an ellipsoid. This ellipsoid may be easily obtained by using a scale drawing of the model to be tested and a set of elliptical templates. The ratios of the axes may therefore be obtained which then allows the use of figures 4 and 6

to obtain the mass and inertia coefficients. The ellipsoid could then be scaled up to the size of the model so that the volume and the moments of inertia may be calculated. Everything needed for the correction equations except the static pressure gradient would be approximated in the above way. The static pressure gradient would be obtained from the survey mentioned above as the slope of the static pressure versus tunnel width evaluated at the center of the tunnel.

The forces and moments needed for the determination of a stability derivative may be obtained by using either a mechanical or a strain gauge balance. In the Stability Wind Tunnel at Virginia Polytechnic Institute and State University the strain gauge balance may be mounted by a strut, through the belly of the body, or by a sting, through the tail. For the mechanical balance to be used, the balance must be mounted by a strut.

A typical test procedure would be as follows:

(1) Approximate the model shape by an ellipsoid of revolution so that the corrections to the forces and moments may be calculated.

(2) Mount the model in the tunnel in any of the above ways.

(3) Measure the forces and moments.

(4) Change the angle of attack and then go to step (3) until the entire range of angles has been accomplished.

(5) Change the angle of sideslip and then go to step (3) until the entire range of angles has been accomplished.

(6) Change the model configuration and then go to step (3) until all of the configurations have been tested.

(7) Remove the model to prevent its damage and to allow a pressure survey of the flow.

(8) Curve the walls and add the proper drag screens to achieve the proper tunnel flow for the tunnel curvature selected. (See Appendix A.)

(9) Survey the flow for the static and total pressure distributions in order that the static pressure gradient used in the corrections and the non-dimensional yawing rate be calculated.

(10) Go to step (2) and repeat the procedure until every value of the selected tunnel curvatures has been tested.

In order to illustrate the above, a 1/11 scale model of a twin engine fighter known as the F-4 was tested in the wind tunnel at Virginia Polytechnic Institute and State University. Some results of this test are presented in Appendix B. This model, shown in figure 7, was the same as that used in references 7 and 8 with the exception of the splitter plate, located between the two engine exhausts, which had to be removed when a hole was bored to provide clearance for the sting.

The sting was mounted in the wind tunnel by a support pylon with "dog-leg" arms (see figure 8) which allowed the angle of attack to range from 0 to 45 degrees while the center of the model remained in approximately the center of the tunnel. Side-slip angles were obtained through the use of a traverse section of the tunnel which moved the pylon across the tunnel and rotated it until the proper angle was obtained. Because of the limitations of the tunnel size the angles of side-slip could only range from -5 to +5 degrees.

The tunnel itself may be classified as a continuous, single return tunnel with a closed test section that is interchangeably round (for the rolling derivatives) or square (for the pitching and yawing derivatives). The round test section contains a rotor at the upstream end as a means of rolling the flow instead of the model to simulate the flow experienced by a rolling body. The square test section is six feet on each side and normally twenty-two feet long with vertical walls, flexible enough so they can be deflected by means of a series of jacks to form the desired curved channel. The velocity variation also requires the use of a combination of drag screens at the upstream end of the tunnel (see Appendix A for the proper screens to be used for each curvature).

This ellipsoid had a semi-length of 30.04 inches, a semi-height of 4.56 inches and a semi-width of 4.89 inches. Consequently the values from figures 4 and 6 were found to be

$$a/c = 6.26 \qquad b/c = 0.95$$

$$K_1 = 0.04 \qquad K_1' = 0$$

$$K_2 = 0.90 \qquad K_2' = 0.8$$

$$K_3 = 0.94 \qquad K_3' = 0.8$$

$$V' = 1.594 \text{ ft}^3$$

Further corrections to those described above were made to the test results. Since the center of volume and the C. G. position of the aircraft was at the same position, no correction was necessary to the derived corrections of the forces and moments. However, there was a

slight misalignment of 6 degrees pitch and 0.18 inches aft in the balance center with respect to the C. G. position. Corrections for blockage were also taken into account. It should be pointed out that if a pitot tube is used to measure the dynamic pressure and thus obtain the velocity of the curved flow, it may or may not give the average value of this pressure. Since the velocity varies throughout the flow the position and direction in which the tube is pointing determines what the pitot tube measures. It is therefore better to make blockage corrections using a constriction pressure ratio as is described in any wind tunnel testing book.[9]

III. ADDITIONAL WIND TUNNEL TESTING TECHNIQUES AS COMPARED TO THE CURVED FLOW TECHNIQUE

There are three primary methods for obtaining dynamic stability derivatives other than the curved flow method. The first two, the whirling-arm method and the method of curved models are not often used since there are important difficulties involved in each. The whirling-arm method, as the name implies, involves a model attached to the end of a beam that rotates about some point. It has been found that difficulties arise in the centrifugal forces and in the complex airflow that is induced around the body.[6] The method of curved models involves the construction of special models for each test curvature. This is of course not economically feasible. The third technique is the oscillation method of which there are two basic types, forced and free. Of these two types, the free oscillation technique is the simplest and the most reliable at angles of attack that are not far greater than the stall angle of attack.

Since the more popular and most feasible of the above methods is the free oscillation method, this comparison will be limited to a comparison of curved flow wind tunnel testing with free oscillation wind tunnel testing. In the free oscillation method, the model is mounted in the tunnel by means of a system of flexure pivots such that it has only one degree of freedom. The model is then deflected and allowed to oscillate while a record of the time and displacement is kept. By connecting the amplitudes of the above time history the period of oscillation and the time to half amplitude may be calculated. The

method would be repeated for wind-on and wind-off conditions so that the contribution from the frictional forces may be subtracted.

The equations of motion for a body are found in reference 1. If we consider, for example, the motion of oscillation in yaw only, the equation of motion for this case becomes

$$\bar{q}_c sb \left(C_{n_{\dot{r}}} \frac{\dot{r}b^2}{2V^2} + C_{n_r} \frac{rb}{2V} + C_{n_{\dot{\beta}}} \frac{\dot{\beta}b}{2V} + C_{n_\beta} \beta\right) + M_\psi \psi = I_z \ddot{\psi} \tag{46}$$

where M_ψ, the moment due to the flexures, is a known quantity. The solution to the above differential is known to be exponential in the form of

$$\psi = \bar{A}e^{\lambda t} \tag{47}$$

where λ has been solved for in reference 1 by substituting 47 into 46.

$$\lambda = \frac{(C_{n_r} - C_{n_{\dot{\beta}}})\frac{b}{2V}}{2\left(\frac{I_z}{\bar{q}_c sb} - \frac{b^2}{4V^2} C_{n_{\dot{r}}}\right)} \pm \frac{\left[(C_{n_r} - C_{n_{\dot{\beta}}})^2 \frac{b^2}{4V^2} - 4\left(\frac{I_z}{\bar{q}_c sb} - \frac{b^2}{4V^2} C_{n_{\dot{r}}}\right)\left(C_{n_\beta} - \frac{M_\psi}{\bar{q}_c sb}\right)\right]^{1/2}}{2\left(\frac{I_z}{\bar{q}_c sb} - \frac{b^2}{4V^2} C_{n_{\dot{r}}}\right)} \tag{48}$$

$$\lambda = a \pm i\omega$$

If one remembers that the time to half amplitude, $t_{\frac{1}{2}}$, is equal to 0.693/a where a is the real part of lambda and that the period, P, is $2\pi/\omega$ where omega is the imaginary part of lambda, then two equations may be written using that information.

At this point, many different methods have been devised by almost as many authors to arrive at an approximation, at least, of the derivatives C_{n_r}, C_{n_β}, $C_{n_{\dot{r}}}$, and $C_{n_{\dot{\beta}}}$. Differences in such parameters as sweep angle, aspect ratio and reference velocity may be used as parameters to classify different approaches to the problem. The problem with this method is which terms can be considered small enough to drop out of the equations and when. In the above analysis the two equations are found to be

$$\frac{(C_{n_r} - C_{n_{\dot{\beta}}}) \frac{b}{2V}}{2\left(\frac{I_z}{q_c sb} - \frac{b^2}{4V^2} C_{n_{\dot{r}}}\right)} = \frac{-0.693}{t_{\frac{1}{2}}} \tag{49}$$

and

$$\frac{\left[(C_{n_r} - C_{n_{\dot{\beta}}}) \frac{b^2}{4V^2} - 4\left(\frac{I_z}{q_c sb} - \frac{b^2}{4V^2} C_{n_{\dot{r}}}\right)\left(C_{n_\beta} - \frac{M_\psi}{q_c sb}\right)\right]^{1/2}}{2\left(\frac{I_z}{q_c sb} - \frac{b^2}{4V^2} C_{n_{\dot{r}}}\right)} \tag{50}$$

In equation 49, the second term in the denominator may usually be considered small when compared to the first term; and in equation 50 the first term under the radical may usually be considered small when compared to the second term. Equations 49 and 50 then become

$$C_{n_r} - C_{n_{\dot{\beta}}} = \frac{-2.772 I_z V}{q_c sb^2 t_{\frac{1}{2}}} \tag{51}$$

$$C_{n_\beta} + \left(\frac{\omega b}{2V}\right)^2 C_{n_{\dot{r}}} = \frac{1}{q_c sb}\left(\omega^2 I_z + M_\psi\right)$$

Equation 51 illustrates the biggest drawback of oscillation tests in that combinations of stability derivatives appear in the equations instead of the stability derivatives alone. Several authors (references 10 and 11) have developed theories for approximating the dynamic stability derivatives separately from each other but at this time, there is no universal method for finding the values of the individual derivatives obtained through oscillation tests to the accuracy obtained by the curved flow technique.[11]

In order to facilitate a comparison of the oscillation technique with the curved flow technique the following statements may be made.

1. Each of these methods requires the same model for testing and differs only in the way in which the model is mounted. In curved flow testing the model is rigidly attached to a balance system while in oscillation testing the model must be free to oscillate.
2. The tunnel used for curved flow testing is a specially designed tunnel with curvable walls and upstream drag screens to attain proper flow characteristics while oscillation testing requires only a standard, straight flow facility.
3. Curved flow requires only the measurement of forces and moments imposed by the flow on the body and not the complete time history of the motion of the body that oscillation testing requires. A complete time history of the motion of the body often requires sensitive measuring apparatus and exacting laboratory technique before any meaningful results may be obtained.

4. The equations of motion involved in the analysis of the data for the oscillation technique are linearized equations (at least to some degree) and will result in errors when the oscillations are extremely large. For this reason, care must be taken that the model does not oscillate at a resonant frequency. This problem may be easily resolved by the addition of masses to the oscillation system.
5. In many cases, such as at high angles of attack, the unsteady effects that are usually neglected in an analysis of the oscillation data may become large and therefore may not be neglected.
6. Once the test is set up, the acquisition of the dynamic stability derivatives takes less wind tunnel time in oscillation testing than in curved flow testing since the process of curving the tunnel walls and adding the upstream drag screens is very time consuming.
7. The dynamic stability derivatives obtained from curved flow testing are not in combination with other dynamic derivatives as they are in oscillation testing.

IV. CONCLUDING REMARKS

Curved flow wind tunnel testing is a useful tool for obtaining the dynamic stability derivatives that are used in an analysis of the stability and control requirements of modern aircraft. As in all other testing procedures, however, there are both advantages and disadvantages to this technique. Of the advantages and disadvantages described in the comparisons in the previous section, the greatest advantage lies in the fact that the derivatives obtained from curved flow testing are not in combination with other derivatives. The greatest disadvantage is the unavailability of a curved flow tunnel. All of the facts presented above should be considered when choosing a method of obtaining dynamic stability derivatives.

Further analysis in this area could be accomplished by the designing and building of the apparatus necessary for oscillation testing in the Stability Wind Tunnel at Virginia Polytechnic Institute and State University. Then the F-4 model that was tested in curved flow for the NASA Langley Research Center (Task Order NAS1-10646-16) and described in this paper could be oscillation tested. The results obtained from the two tests of the same model in the same wind tunnel could then be compared with each other and with results from actual flight test data of this aircraft.

V. LITERATURE CITED

[1]Queijo, M. J., "Methods of Obtaining Stability Derivatives," NASA Special Publication, No. 258, 1971, pp. 71-101.

[2]Bird, John D., Jaquet, Byron, M. and Cowan, John W., "Effect of Fuselage and Tail Surfaces on Low-Speed Yawing Characteristics of a Swept-Wing Model as Determined in Curved-Flow Test Section of Langley Stability Tunnel," NACA Technical Note, No. 2483.

[3]Taylor, G. I., "The Forces on a Body Placed in a Curved or Converging Stream of Fluid," Proceedings of the Royal Society, Vol. 120, 1928, pp. 260-283.

[4]Lamb, Sir Horace, Hydrodynamics, Dover Publications, New York, New York, 1945.

[5]Donlan, C. J., "A Comparison of the Forces and Moments Acting on a Body (1) Moving in a Circular Path Through a Fluid at Rest (Flight) and (2) Held at Rest in a Fluid that is Moving in a Circular Path," NACA Memorandum For Files, No. L3F01.

[6]Bird, John D., Lichtenstein, Jack H. and Jaquet, Byron M., "Calibration of Curved Flow Test Section of Stability Wind Tunnel," NACA Memorandum for Files.

[7]Chambers, Joseph R. and Anglin, Ernie L., "Analysis of Lateral-Directional Stability Characteristics of a Twin-Jet Fighter at High Angles of Attack," NASA Technical Note, No. D5361, 1969.

[8]Anglin, Ernie L., "Static Force Tests of a Model of a Twin-Jet Fighter Airplane for Angles of Attack from -10° to 110° and Sideslip Angles from -40° to 40°," NASA Technical Note, No. D6425, 1971.

[9]Pope, Alan and Harper, John S., Low Speed Wind Tunnel Testing, John Wiley and Sons, Inc., New York, New York, 1966.

[10]Rodden, William P. and Giesing, Joseph P., "Application of Oscillatory Aerodynamic Theory to Estimation of Dynamic Stability Derivatives," Journal of Aircraft, Vol. 7, No. 3, 1970, pp. 272-275.

[11]Campbell, John P. and McKinney, Marion O., "Summary of Methods for Calculating Dynamic Lateral Stability and Response and for Estimating Lateral Stability Derivatives," NACA Report, No. 1098.

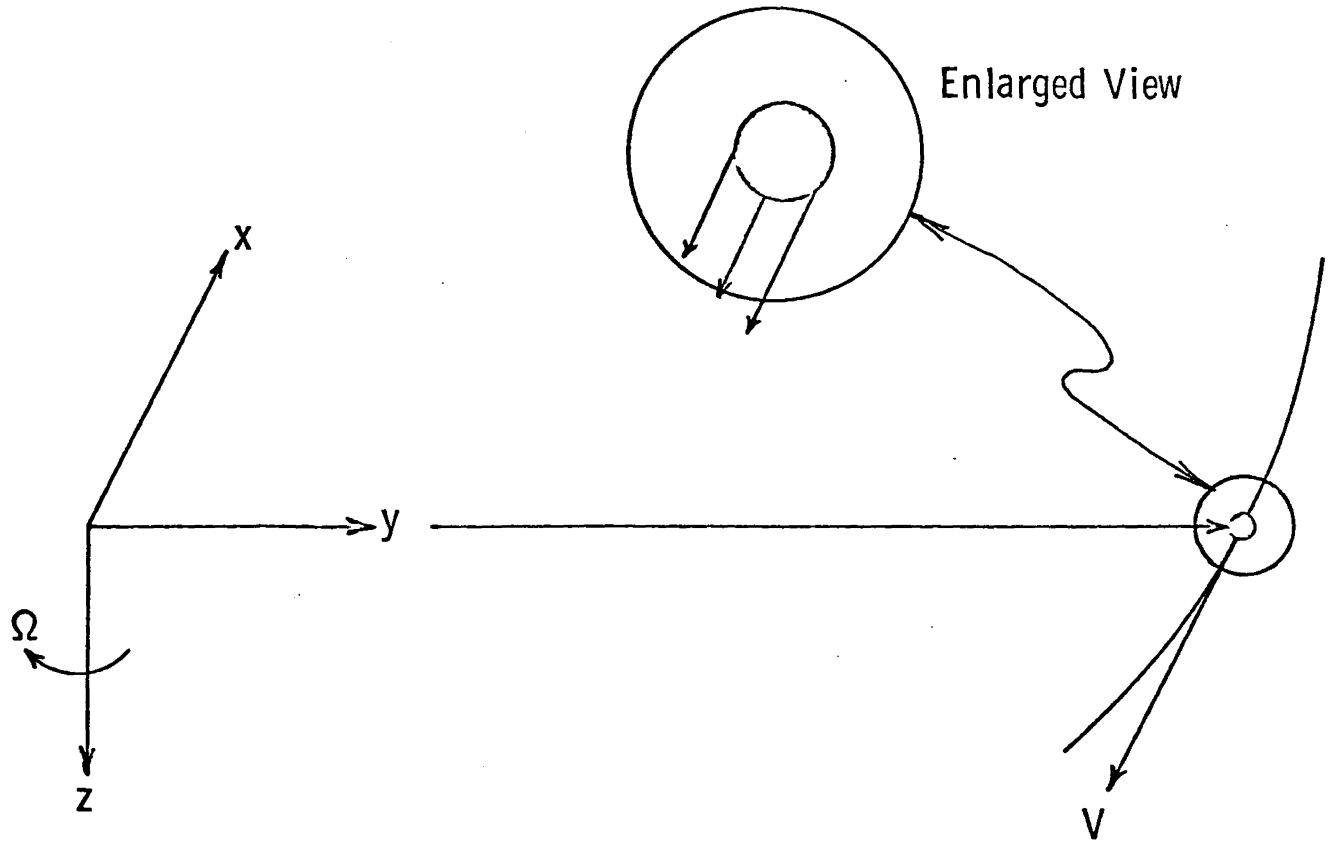

Figure 1 The Inertial Axis System for Curved Flow

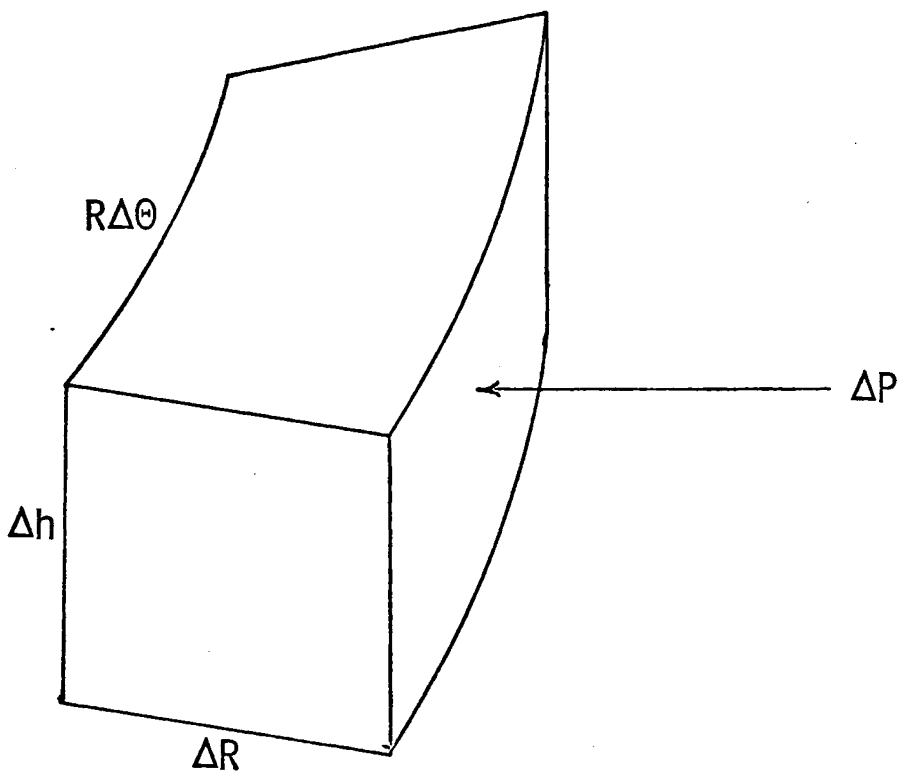

Figure 2 The Fluid Element in Curved Flow

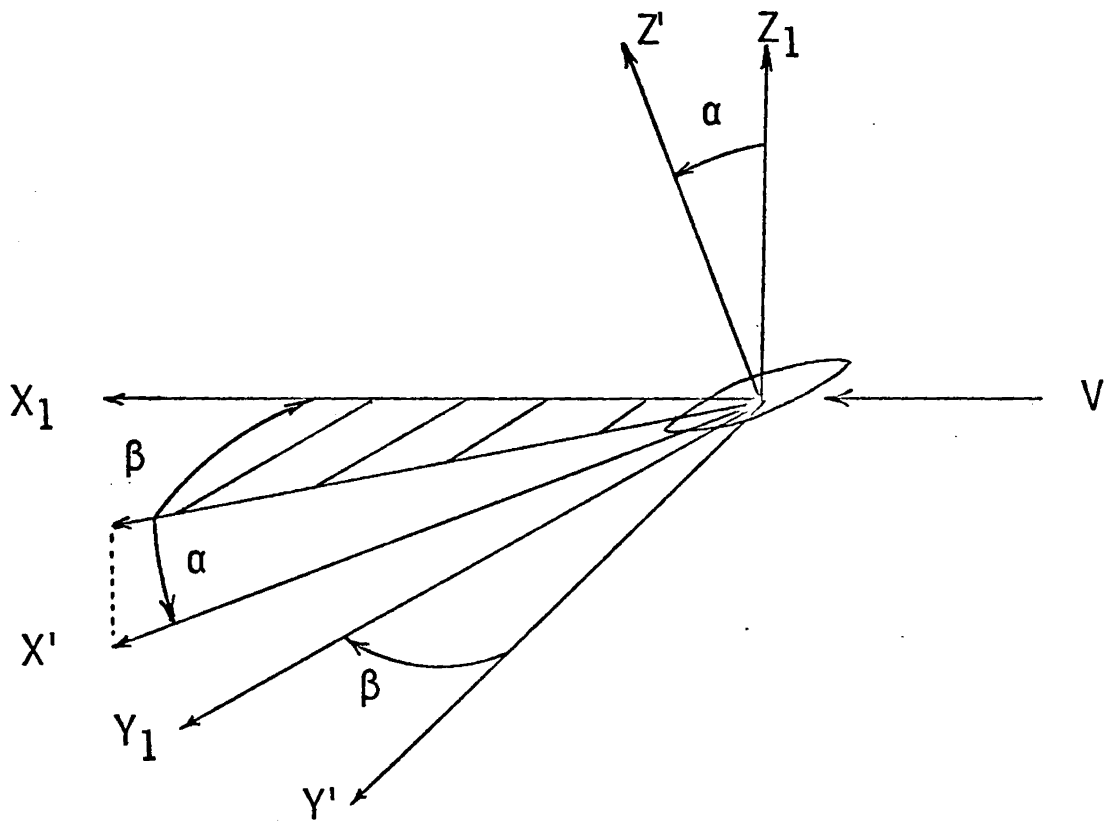

Figure 3 The Body Axis System for Curved Flow

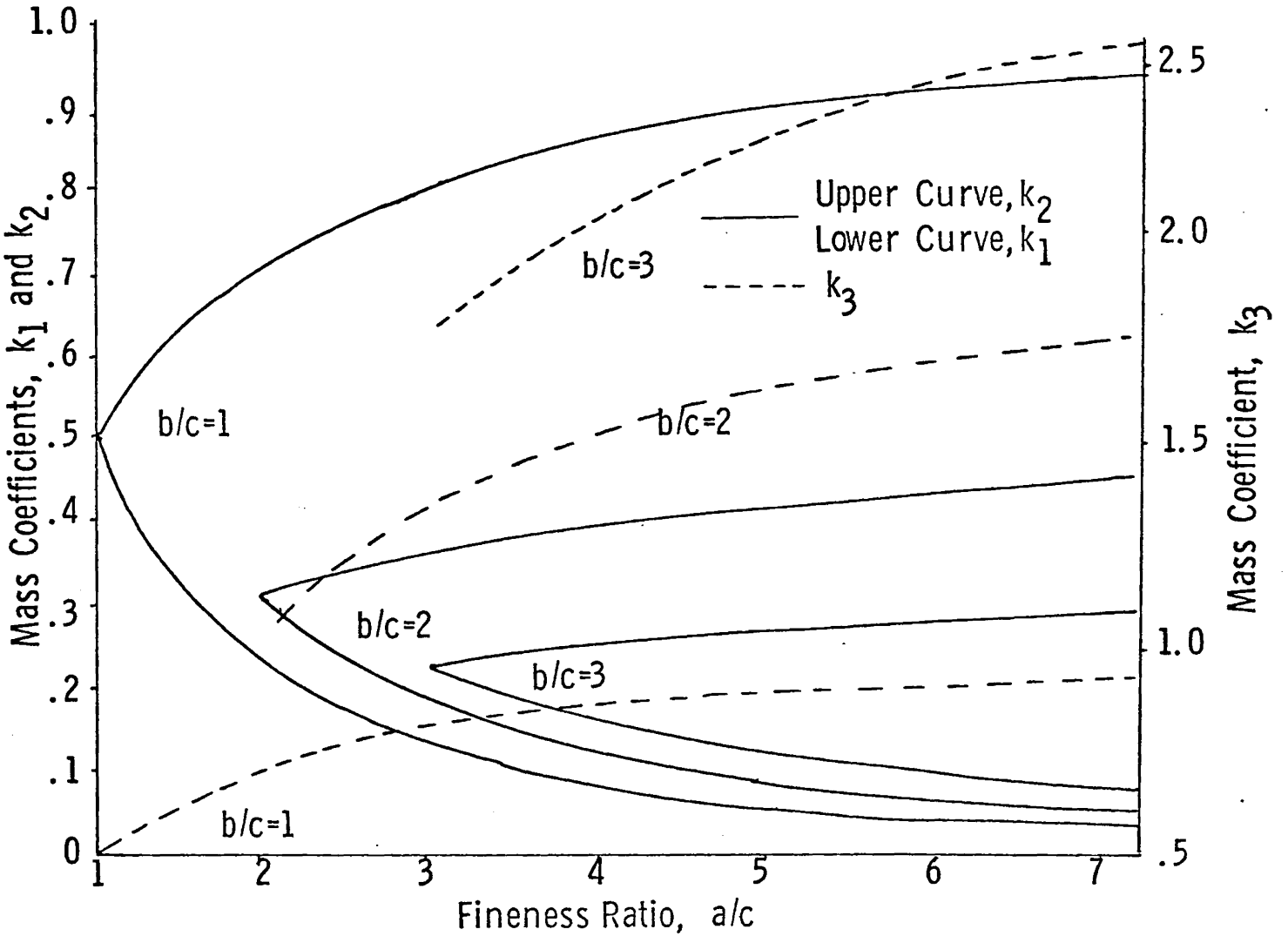

Figure 4 Mass Coefficients for Ellipsoids of Revolution

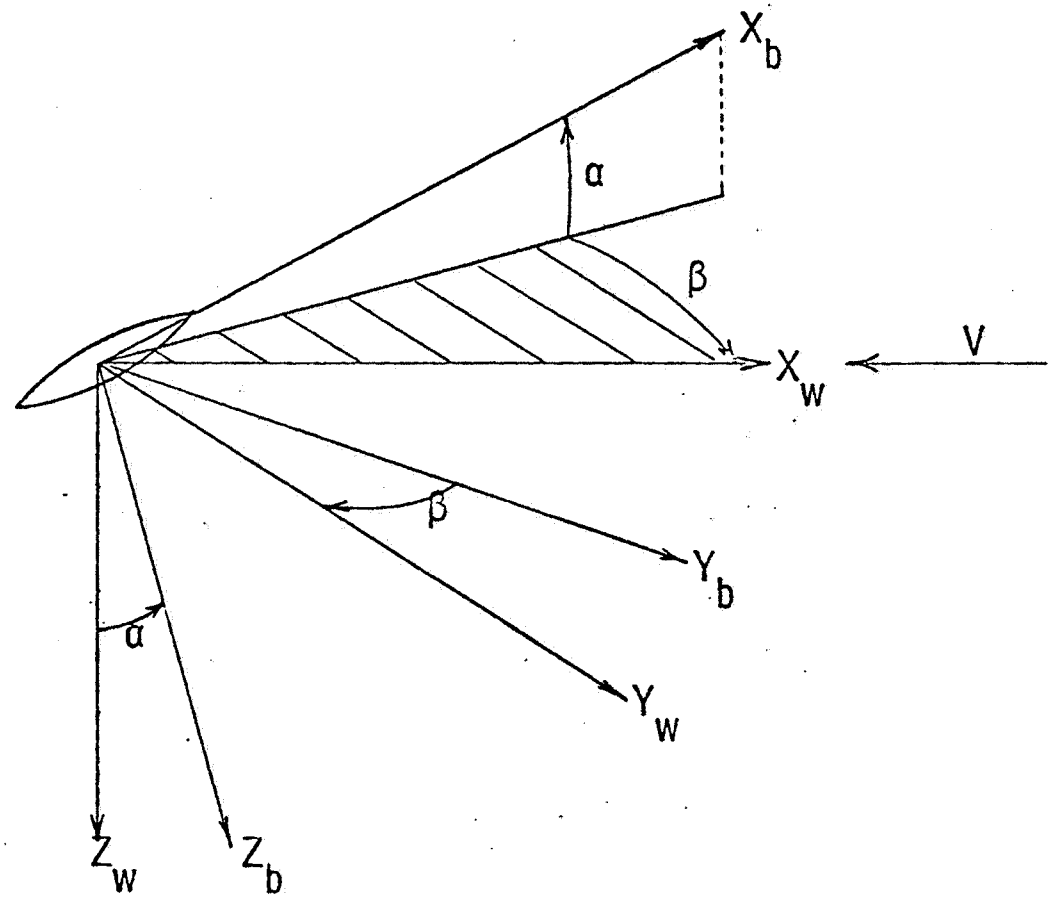

Figure 5 The Body Axis System for Curved Flight

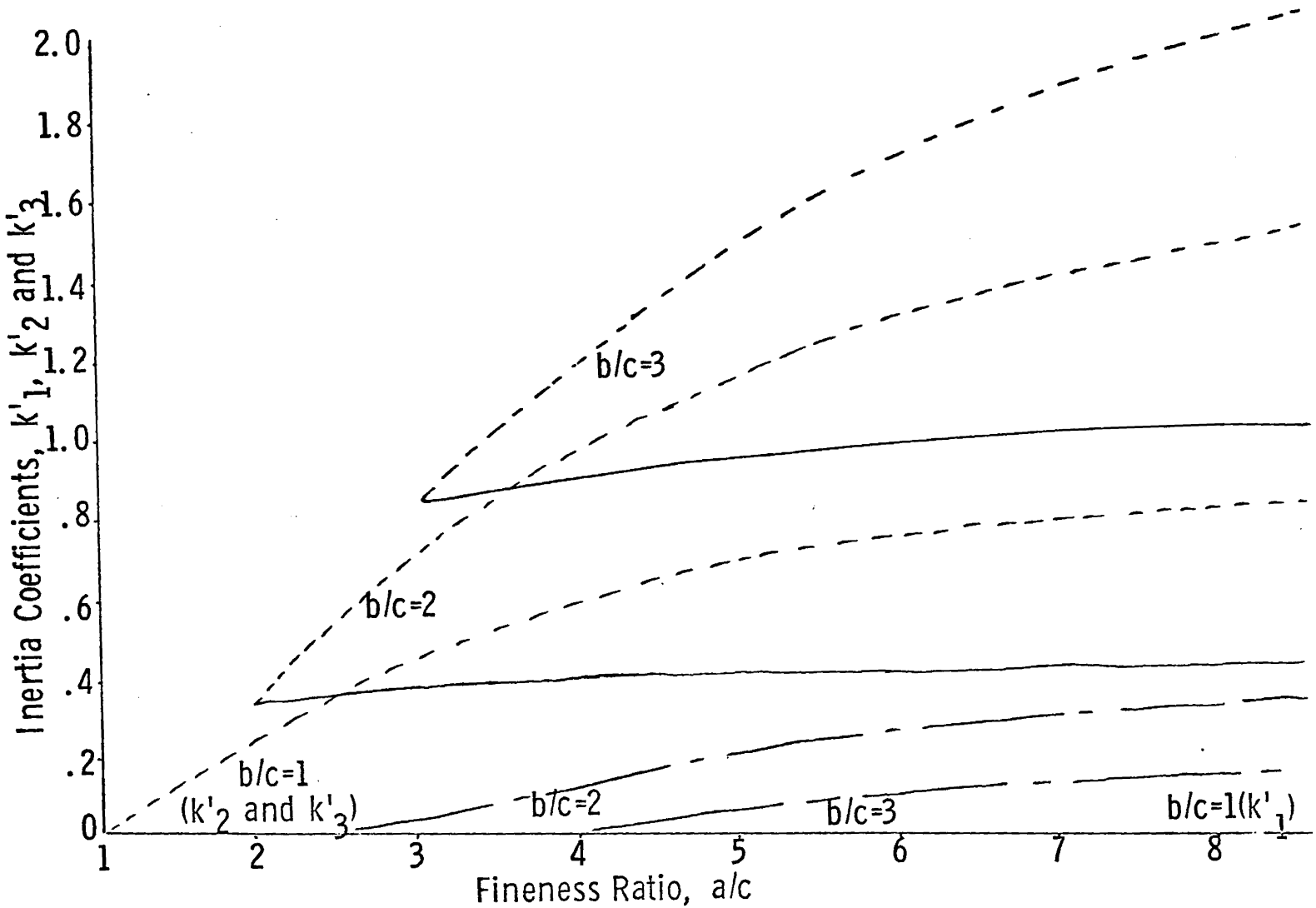

Figure 6 Inertia Coefficients for Ellipsoids of Revolution

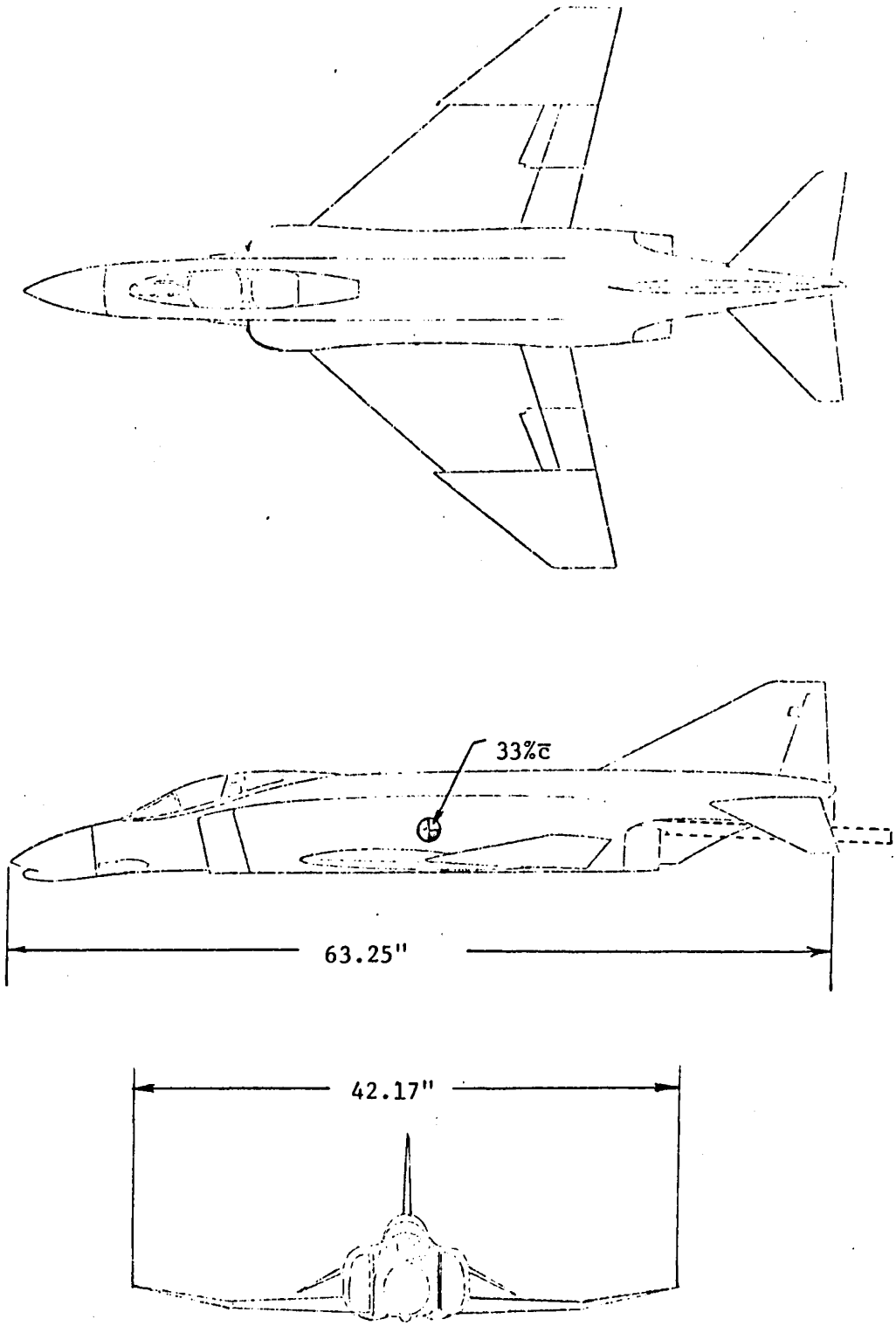

Figure 7 A Three View Sketch of the F-4 Model

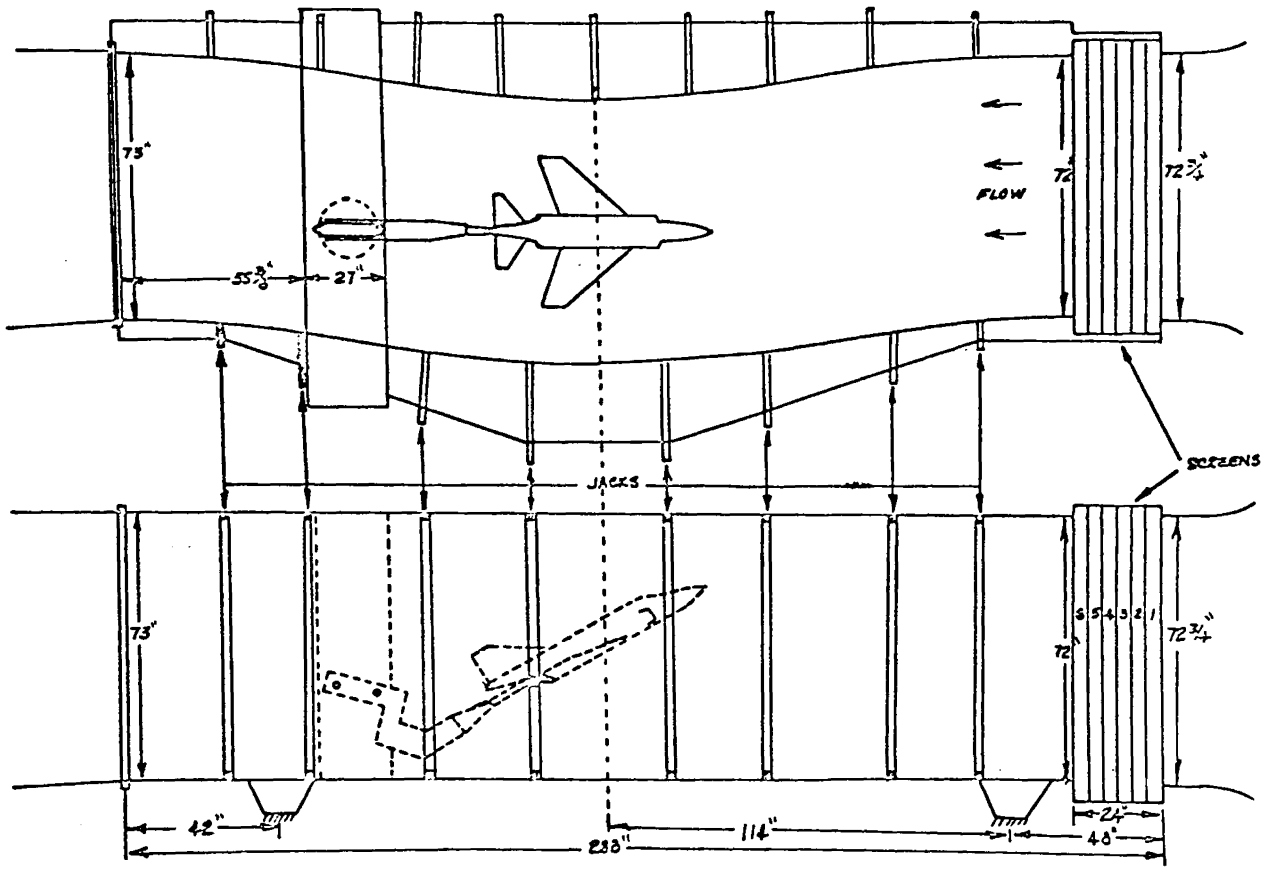

Figure 8 Curved Flow Test Section

APPENDIX A

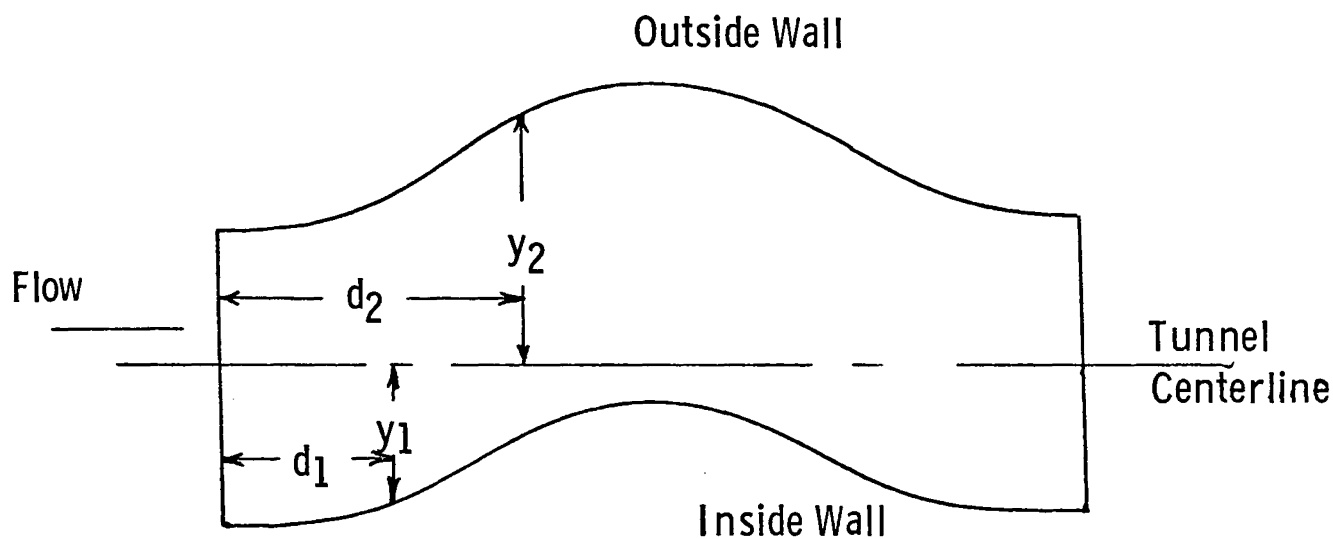

Figure A-1 Plan View of Curved Flow Tunnel

Table A-1

Screens 1, 2

$\hat{r}$ = .0372, $\overline{q}_c$ = 8 psf. $\hat{r}$ = .0415, $\overline{q}_c$ = 25 psf.

$\hat{r}$ = .0394, $\overline{q}_c$ = 16 psf. $\hat{r}$ = .0460, $\overline{q}_c$ = 40 psf.

	Inside Wall		Outside Wall	
Station	distance, d_1	deflection, y_1	distance, d_2	deflection, y_2
1	26.25"	35.40"	29.25"	37.00"
2	54.62	33.20	58.69	40.00
3	82.81	29.60	84.81	43.10
4	106.19	27.65	114.50	45.10
5	132.00	26.90	132.00	45.40
6	157.81	27.80	149.62	45.40
7	183.62	30.10	179.25	43.20
8	209.38	33.35	205.44	40.20
9	236.50	35.55	235.31	37.15

Table A-2

Screens 1, 2, 3

$\hat{r} = 0.055$, $\overline{q}_c = 8$ psf. $\hat{r} = .0689$, $\overline{q}_c = 25$ psf.

$\hat{r} = 0.622$, $\overline{q}_c = 16$ psf. $\hat{r} = .0727$, $\overline{q}_c = 40$ psf.

	Inside Wall		Outside Wall	
Station	distance, d_1	deflection, y_1	distance, d_2	deflection, y_2
1	26.25"	35.12"	29.25"	37.50"
2	54.62	32.38	58.69	41.88
3	82.81	27.06	84.81	46.19
4	106.19	24.12	114.50	48.81
5	132.00	23.12	132.00	49.25
6	157.81	24.19	149.62	48.88
7	183.62	27.62	179.25	46.31
8	209.38	32.19	205.44	42.00
9	236.50	35.25	235.31	37.62

Table A-3

Screens 1, 2, 3, 4

$\hat{r}$ = .0725, $\overline{q}_c$ = 8 psf. $\hat{r}$ = .080, $\overline{q}_c$ = 25 psf.

$\hat{r}$ = .0813, $\overline{q}_c$ = 16 psf.

	Inside Wall		Outside Wall	
Station	distance, d_1	deflection, y_1	distance, d_2	deflection, y_2
1	26.25"	34.80"	29.25"	38.13"
2	54.62	30.50	58.69	44.62
3	82.81	23.62	84.81	50.48
4	106.19	19.30	114.50	53.98
5	132.00	17.70	132.00	54.53
6	157.81	19.35	149.62	54.08
7	183.62	24.47	179.25	50.63
8	209.38	30.80	205.44	44.82
9	236.50	34.95	235.31	38.28

Table A-4

Screens 1, 2, 3, 4, 5

$\hat{r}$ = .1142, $\overline{q}_c$ = 16 psf.

	Inside Wall		Outside Wall	
Station	distance, d_1	deflection, y_1	distance, d_2	deflection, y_2
1	26.25"	34.40"	29.25"	38.85"
2	54.62	29.30	58.69	47.75
3	82.81	20.20	84.81	55.10
4	106.19	14.25	114.50	59.55
5	132.00	12.80	132.00	60.25
6	157.81	14.35	149.62	59.60
7	183.62	21.20	179.25	55.30
8	209.38	29.50	205.44	47.90
9	236.50	34.60	235.31	39.10

Table A-5

Screens 1, 2, 3, 4, 5

$\hat{r}$ = .1159, $\overline{q}_c$ = 25 psf.

	Inside Wall		Outside Wall	
Station	distance, d_1	deflection, y_1	distance, d_2	deflection, y_2
1	26.25"	34.40"	29.25"	39.00"
2	54.62	29.15	58.69	48.15
3	82.81	19.80	84.81	55.70
4	106.19	13.60	114.50	60.25
5	132.00	11.30	132.00	60.95
6	157.81	13.70	149.62	60.30
7	183.62	20.80	179.25	55.85
8	209.38	29.25	205.44	48.30
9	236.50	34.60	235.31	39.20

Table A-6

Screens 1, 2, 3, 4, 5, 6

$\hat{r}$ = .1409, $\overline{q}_c$ = 16 psf.

	Inside Wall		Outside Wall	
Station	distance, d_1	deflection, y_1	distance, d_2	deflection, y_2
1	26.25"	34.30"	29.25"	39.25"
2	54.62	28.70	58.69	49.20
3	82.81	20.00	84.81	56.00
4	106.19	12.95	114.50	61.05
5	132.00	9.70	132.00	62.60
6	157.81	12.60	149.62	61.60
7	183.62	20.55	179.25	56.60
8	209.38	28.96	205.44	49.30
9	236.50	34.45	235.31	39.40

APPENDIX B

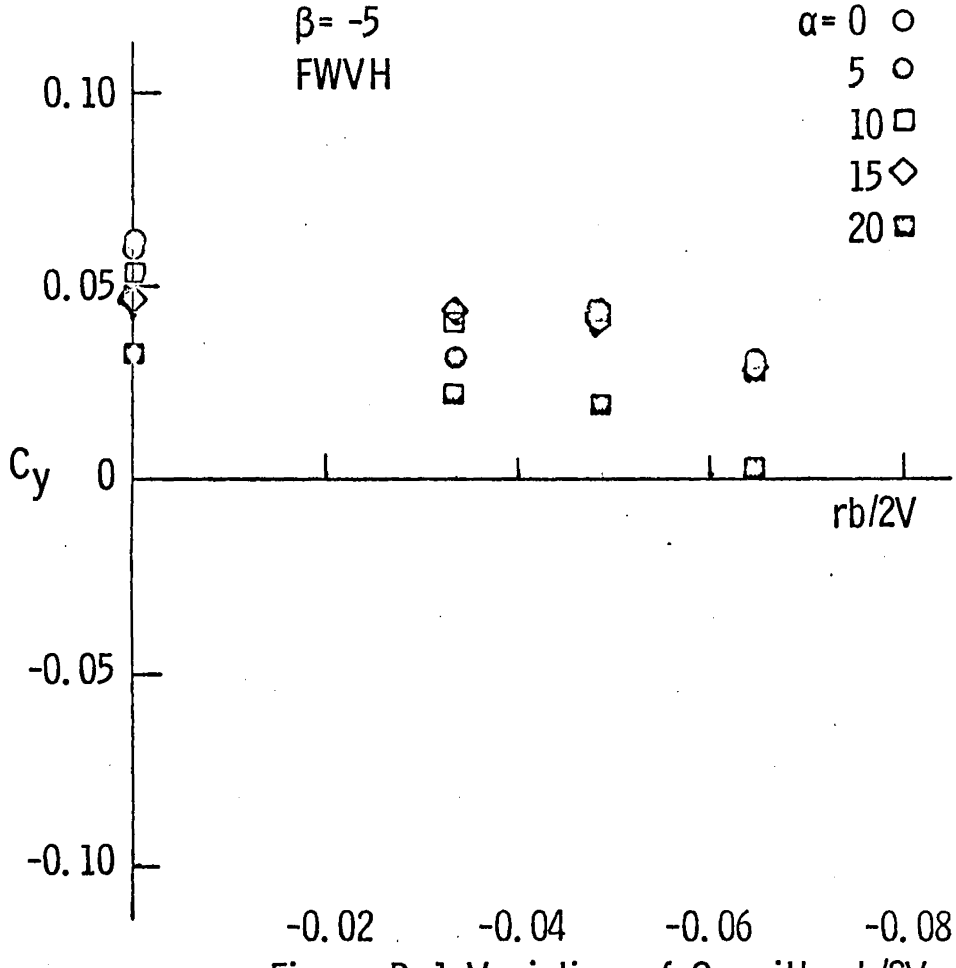

Figure B-1 Variation of C_y with rb/2V

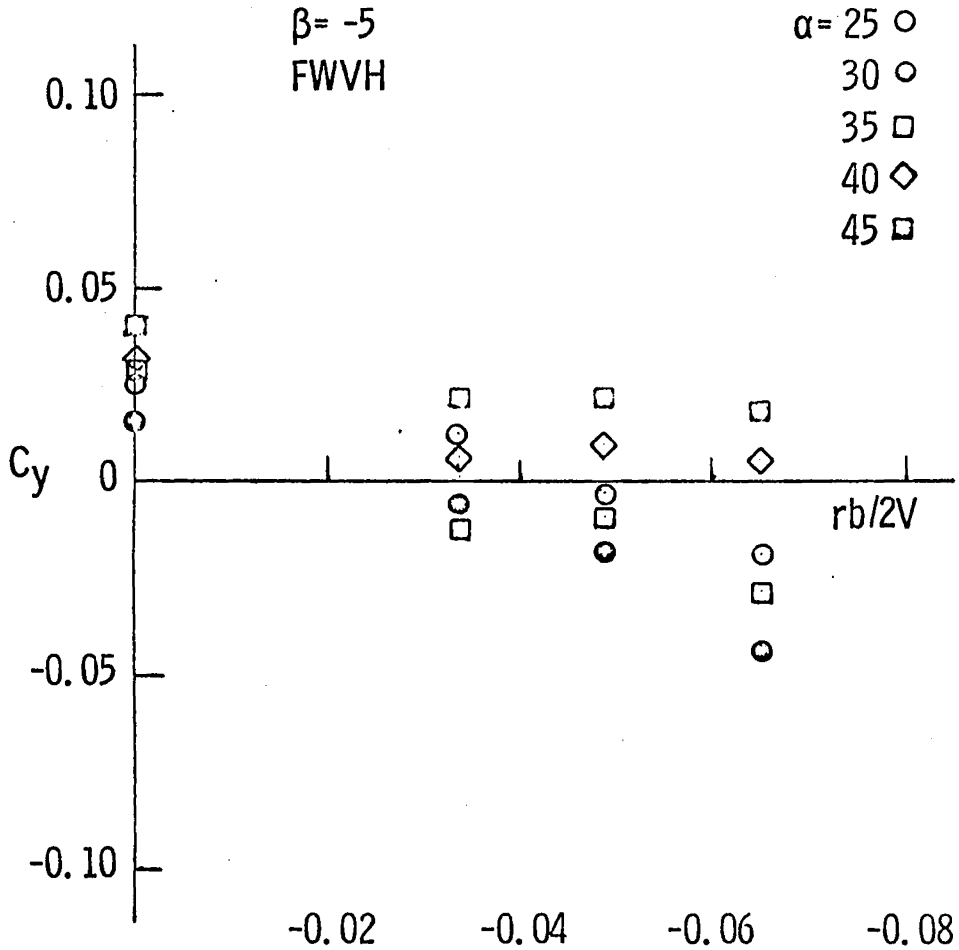

Figure B-2 Variation of C_y with rb/2V

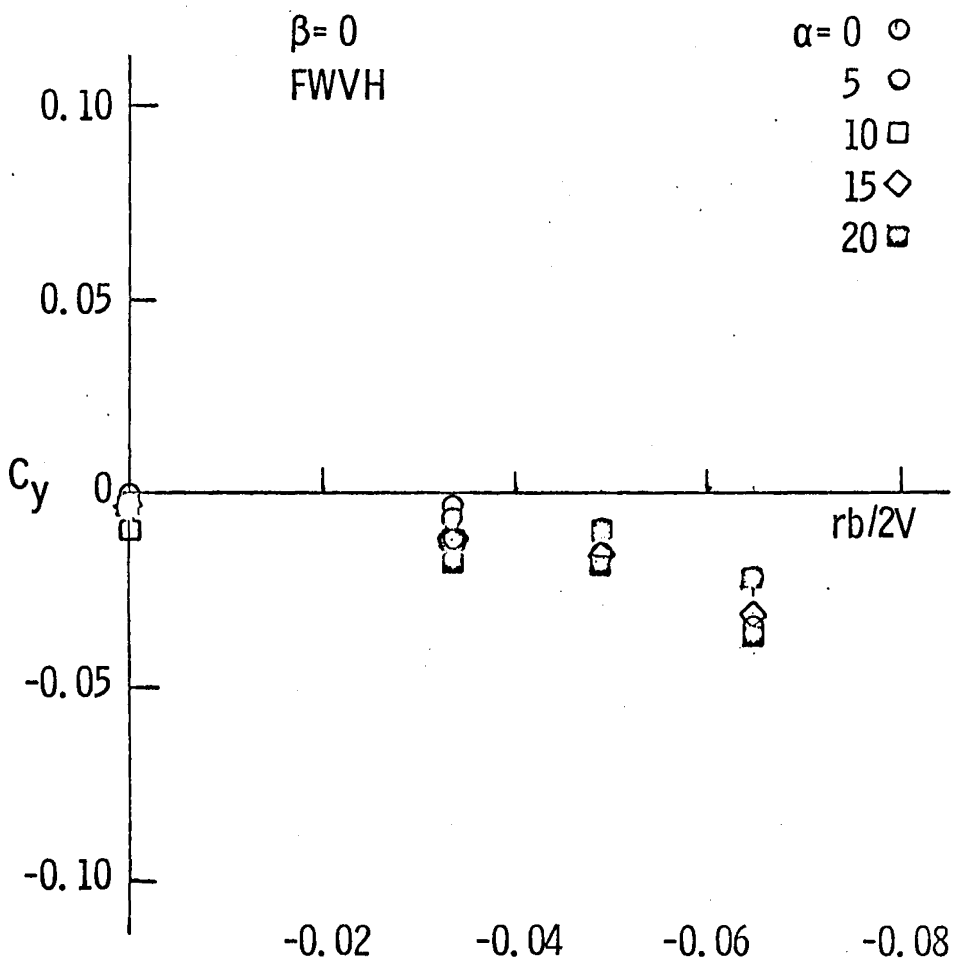

Figure B-3 Variation of C_y with rb/2V

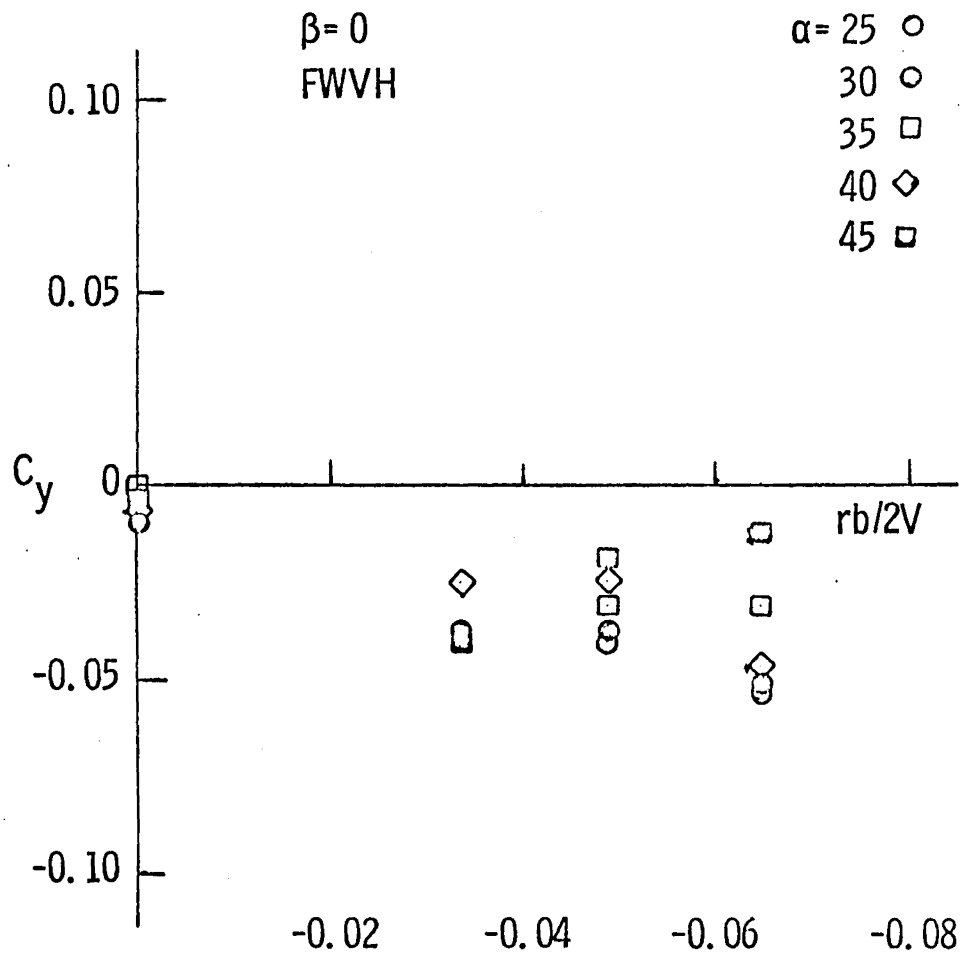

Figure B-4 Variation of C_y with rb/2V

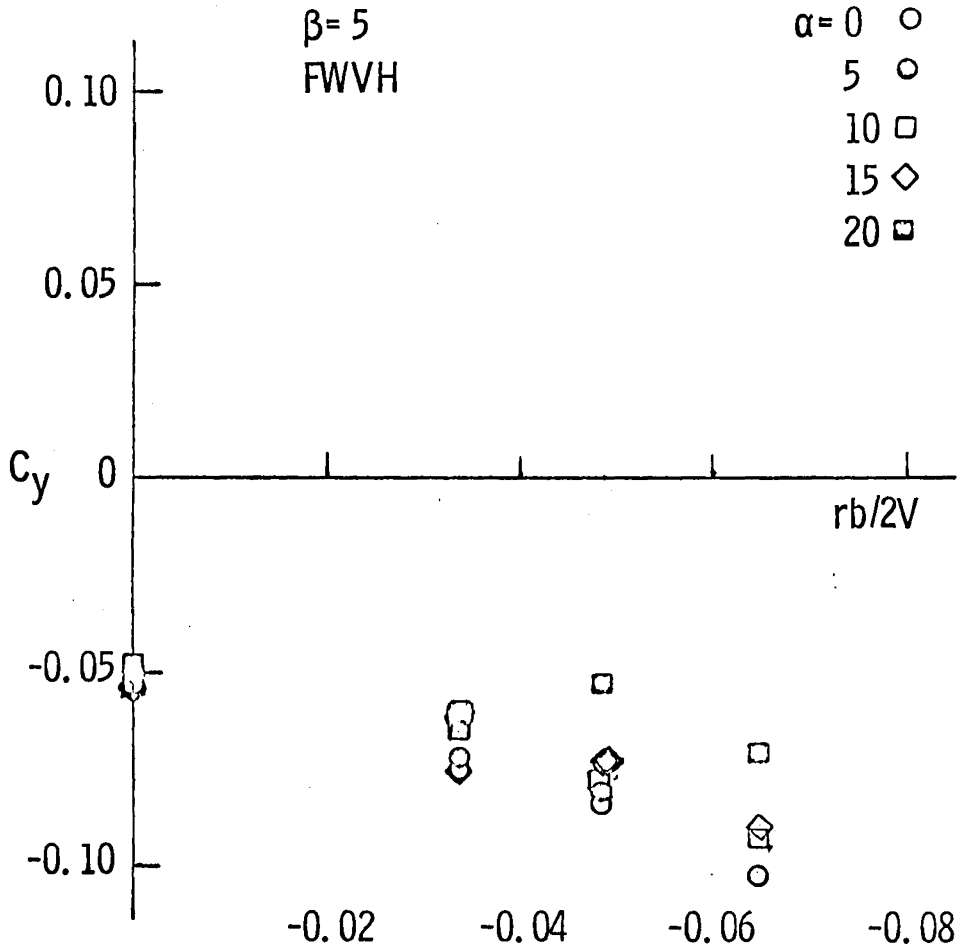

Figure B-5 Variation of C_y with rb/2V

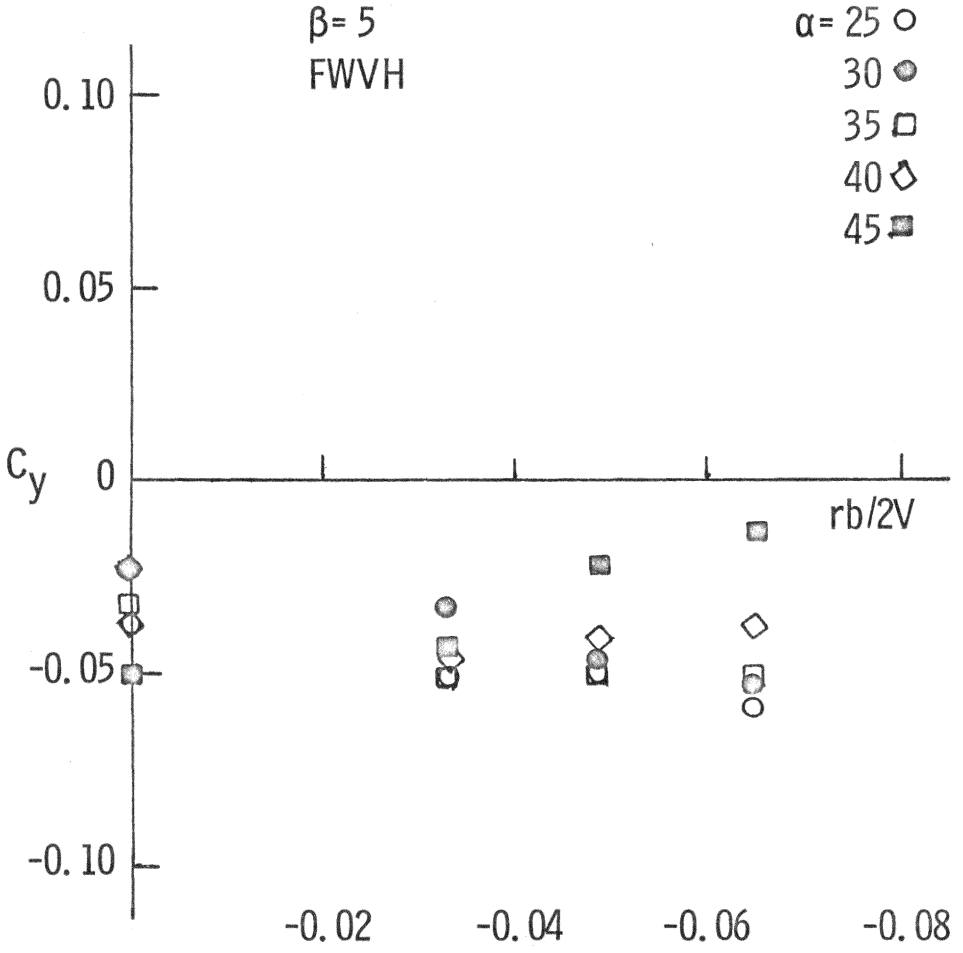

Figure B-6 Variation of C_y with rb/2V

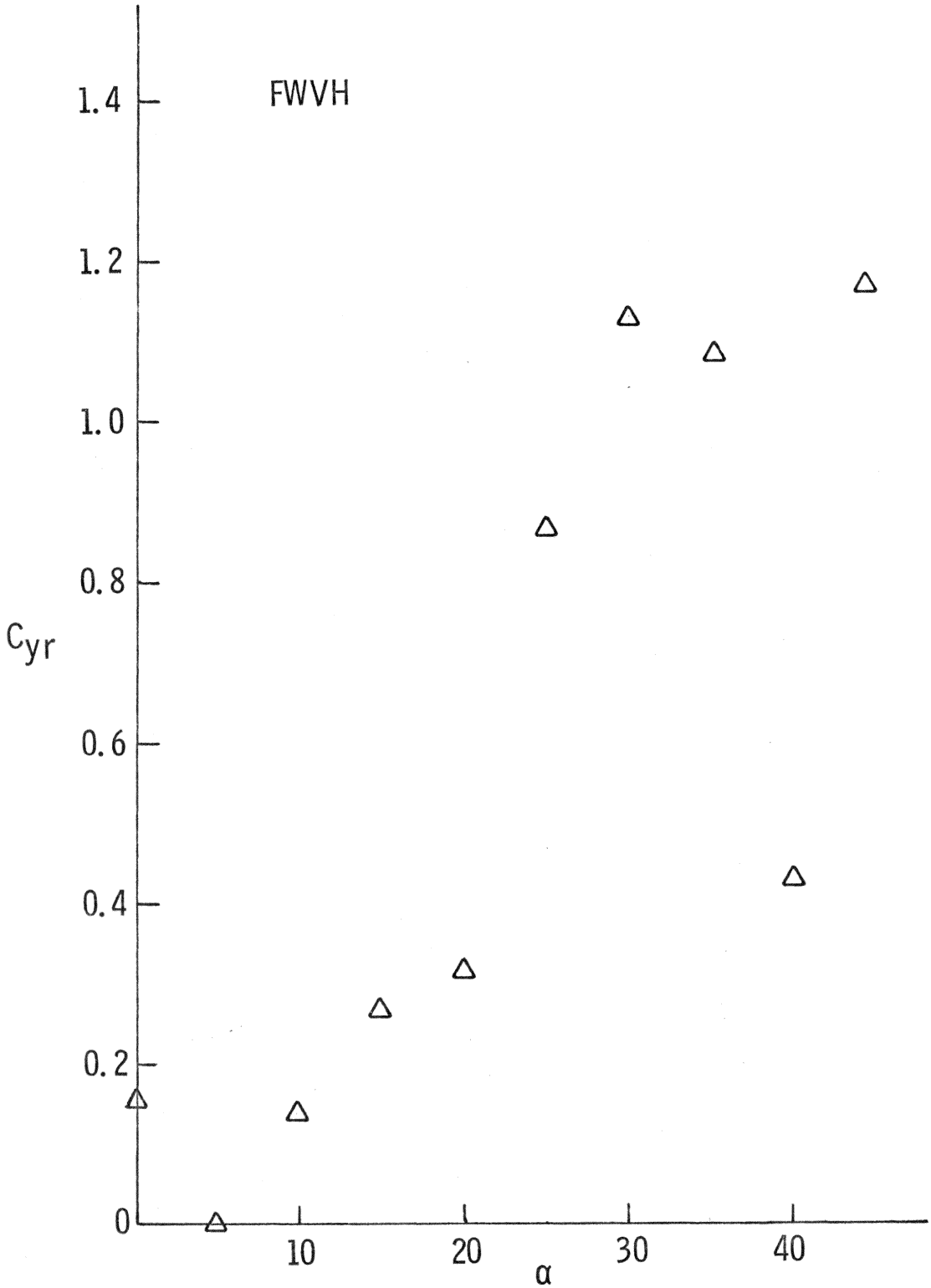

Figure B-7 Variation of C_{yr} with Angle of Attack

The vita has been removed from the scanned document

AN ANALYSIS OF CURVED FLOW WIND TUNNEL TESTING

by

Mack Steele Mutchler

(ABSTRACT)

The theory used to develop curved flow as a method of obtaining dynamic stability derivatives is presented including an analysis of the flows involved in the curved flow wind tunnel and in curved flight. Equations for the forces and moments for each of these flows are presented and then used to develop equations for the corrections to the forces and moments obtained in curved flow wind tunnel tests. An example of the physical setup and of the testing procedure for curved flow testing is also presented with some of the results from a typical test.

The principles involved in several other methods of testing that are also used to obtain the dynamic stability derivatives are discussed so that a comparison may be made with the curved flow method.